Journal of the Korean Physical Society, Vol. 55, No. 4, October 2009, pp. 1389∼1393

Measurements of the Neutron Scattering Spectrum from ^{238}U and Comparison of the Results with a Calculation at the 36.68-eV Resonance

Tae-Ik Ro*
Department of Physics, Dong-A University, Busan 604-714

Yaron Danon,† Emily Liu and Devin P. Barry
Department of Nuclear Engineering, Rensselaer Polytechnic Institute, NY 12180

Ron Dagan
Institut für Reaktorsicherheit (IRS), Forschungszentrum Karlsruhe Gmbh, 3640-76021

(Received 8 June 2009, in final form 22 July 2009)

Neutrons elastically scattered from ^{238}U were measured in the neutron energy region from 5 to 120 eV by using a Ta target with the 60-MV electron linear accelerator (LINAC) of RPI (Rensselaer Polytechnic Institute). The neutron energy, having a continuous spectrum, was measured by using the neutron time-of-flight (TOF) method and a ^{6}Li scintillation detector. Two different thickness depleted uranium samples, 169 and 362 g of 7.62 × 7.62 cm^2, were used in the experiments. The spectra of scattered neutrons were measured at 25.5 m from the U sample by using a ^{6}Li detector, and the scattering direction was ∼39° forward from the direction of the incident neutrons. The peaks and the dips around resonance energy of the measured spectrum were identified and compared to the ENDF/B-VII.0 cross-section of 238U for the same neutron energy. The experimental 36.68-eV resonance was compared with the calculation results. The experimental and the calculation results can be used as reference data for benchmarking neutron scattering models in simulation codes.

PACS numbers: 24.10.v, 28.20.Cz, 29.25.Dz, 29.30.Hs
Keywords: Elastic neutron scattering, Resonance, Time-of-flight, Depleted uranium, LINAC experiment
DOI: 10.3938/jkps.55.1389

I. INTRODUCTION

Neutron scattering on ^{238}U is very important for nuclear technology, such as the design of reactors, so the neutron total and capture cross sections have been measured many times [1]. The last measured fast neutron data for ^{238}U for elastic and inelastic scattering to the first excited level by Miura et al. [2,3] contributed to reducing uncertainties in the measured data and to improving the theoretical models applied for ^{2}38U data analysis. Asghar *et al.* [4] obtained the scattering resonance areas of many resonances. For low neutron energy, the 6.67-eV ^{238}U resonance was studied by Staveloz et al. [5]. Enik *et al.* [6] carried out measurements by using the Dubna booster IBR-30 and a neutron spectrometer UGRA, and discussed three low-energy resonances, 6.67, 20.87, and 36.68 eV. The aim of this experiment is to present the neutron spectrum of elastic scattering from ^{238}U in the energy range from ∼5 to ∼120 eV and to compare the experimental 36.68-eV resonance area with the calculated results. The MCNP [7] code is a famous Monte Carlo transport code, but was not used in this work. Monte Carlo methods are very different from deterministic transport methods. In the deterministic simulation, the ideal-gas-based kernel for scatterers with internal structure was introduced by Rothenstein *et al.* [8–10]. The results of the experiments and calculations are used as reference data for benchmarking neutron scattering models in the MCNP simulation code.

II. EXPERIMENTAL PROCEDURE

In this experiment, the scattering measurements were carried out using the Gaerttner electron linear accelerator at Rensselaer Polytechnic Institute (RPI), which is operated at ∼55 MeV with a pulse repetition rate of 100 Hz, an electron pulse width of 0.2 μs, and an average electron current of 60 μA . The pulsed electron beam im-

*E-mail: tiro@dau.ac.kr; Fax: 051-200-7232;
†E-mail: danony@rpi.edu

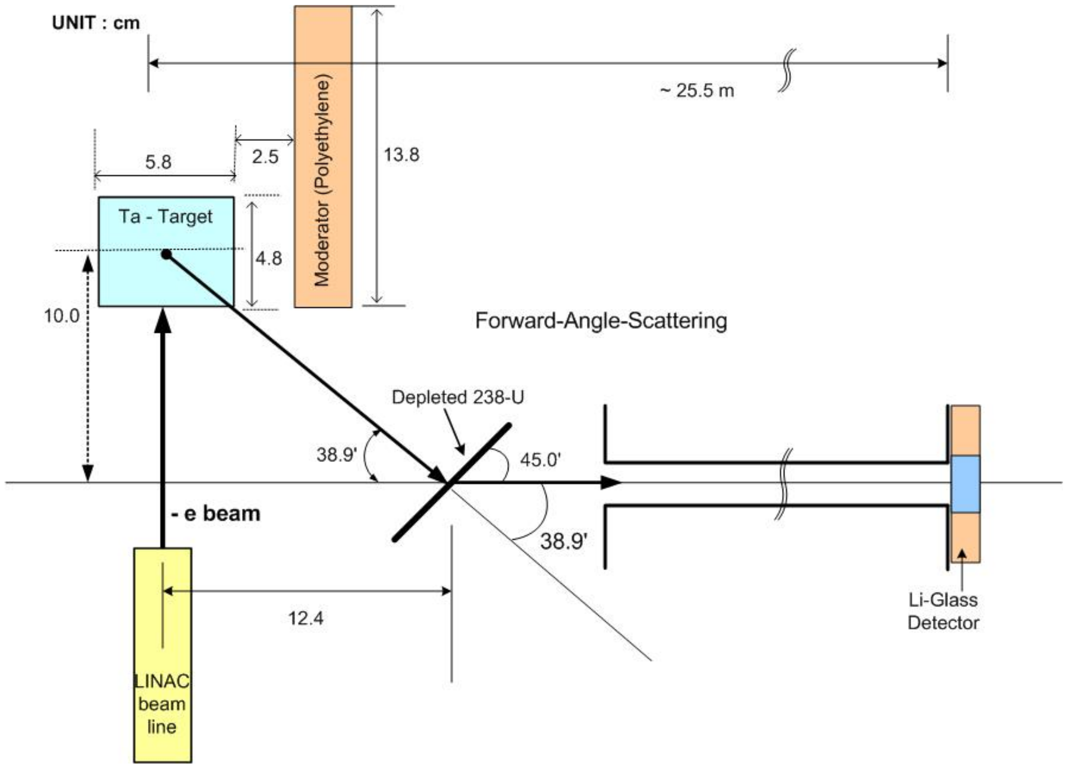

Fig. 1. The geometry of the forward scattering experiment.

pinges upon a water-cooled tantalum target, in which the electrons are slowed down and produce bremsstrahlung radiation. This bremsstrahlung radiation then interacts with the tantalum and generates photoneutrons. The resulting pulsed neutron source is moderated with a 2.54-cm-thick piece of polyethylene. The experimental arrangement is described in Fig. 1. The tantalum target produces a white source of neutrons. The neutrons were in the energy range from 5 to 120 eV. The depleted ^{238}U sample for the forward scattering angle measurement is placed about 18.5 cm away from the pulsed neutron source, and the neutrons scattered from this sample drift down an evacuated flight tube to a detector located ~25.5 m away from the e-beam axis. The neutron detector used had a 12.7-cm-diameter by 1.27-cm-thick Bicron GS-20 ^{6}Li-loaded scintillator glass (6.6% lithium, enriched in ^{6}Li to 95%) detector with a Phillips XP4512B photomultiplier. This detector has an efficiency that varies as $1/\nu$ (where ν is the neutron velocity) in this energy range. The product of the neutron flux shape $\phi(E)$ and the detector efficiency $\eta(E)$ was measured by using a lead sample, for which the elastically scattered neutrons have an energy very close to the incident energy. In the energy range from ~5 to ~120 eV, the product behaves like $\phi(E)\eta(E) = CE^p$, where C is a normalization constant and $p = -1.2$.

Two different thickness depleted uranium, with 0.3% U-235, samples were used in the experiments. The impurity did not affect the results because the scattering cross-section at the 36.68 eV resonance is much higher than that of U-235. The characteristics of these samples are found in Table 1. Several measurements were performed for each sample, for the foreground and the background runs.

III. DATA ANALYSIS

The neutron forward scattering TOF spectra observed with the ^{6}Li glass detector for the 169-g and the 362-g samples are shown in Fig. 2. The gamma flash (*gflash*) was located on channel 4^{th}, and the channel width (dt) was 0.256 ns. After subtracting a background, the TOF spectrum was converted to the energy spectrum by the using $E_i = [K \cdot L/(i - gflash) \cdot dt]^2$, where E is the neutron energy (eV), i is the channel number, K = 72.3, L = 25.65 m and $dt = 0.256$ ns. In the TOF spectrum, the 100^{th} channel is 5.694 keV, and the 4000^{th} channel is 3.286 eV.

The energy spectra of the forward scattering runs are shown in Fig. 3. in the energy range from 3.286 to 120 eV. The 120-eV upper energies, which have bad statistical errors, were cut in this graph. We can find evidence for eight dips of resonances (Table 2) at 6.67, 20.87, 36.68, 66.03, 80.74, 89.24, 102.56, and 116.89 eV in Fig. 3. The eight arrows point to the 8 dips in the resonance energy in Fig. 3. Four dips (2, 3, 4, 7) are located near sharp peaks. Due to strong competition with radiative

Table 1. Charateristics of the depleted ^{238}U sample.

Sample ID	Width (cm)	Height (cm)	Thickness (cm)	Weight (g)
Thin	7.62 ± 0.05	7.62 ± 0.05	0.154	169 ± 0.5
Thick	7.62 ± 0.05	7.62 ± 0.05	0.329	362 ± 0.5

Table 2. Resonant neutron energy and total cross-section of ^{238}U.

No.	1	2	3	4	5	6	7	8
Energy (eV)	6.673	20.871	36.685	66.034	80.747	89.246	102.565	116.895
Cross Section (barn)	7579.39	9889.87	13399.5	4360.81	280.096	21.2645	6048.86	2021.04

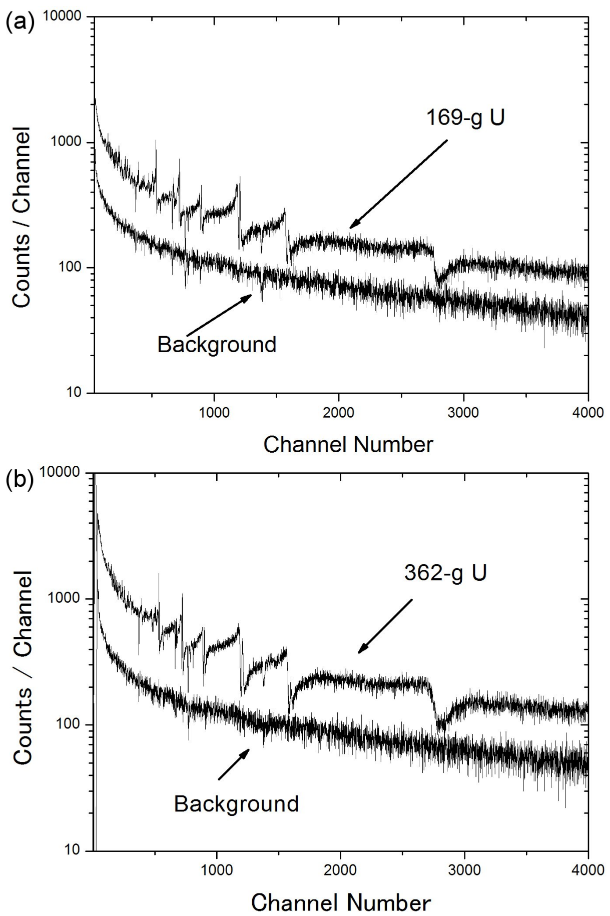

Fig. 2. Neutron TOF spectra for the forward scattering from U samples: (a) 169-g sample and (b) 362-g sample.

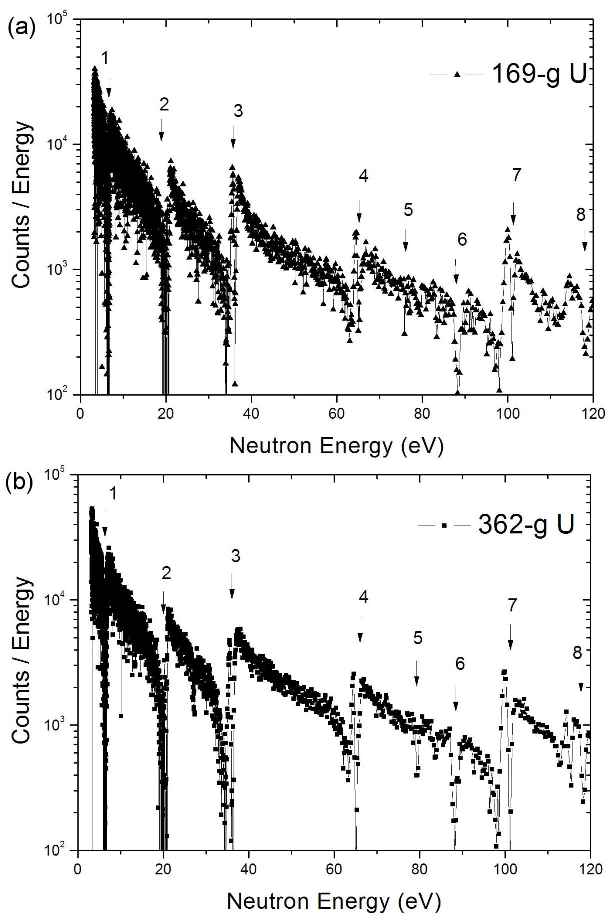

Fig. 3. Neutron scattering energy spectra for the (a) 169-g and the (b) 362-g U samples.

capture, four resonances (1, 5, 6, 8) look very weak even in comparison with potential scattering, nevertheless the resonant dips are easily identified. The peaks are caused by elastically scattered from the U sample. The 36.68-eV resonance peak is shown clearly, and this peak will be compared with the calculated results in the next section. Fig. 4. shows the eight resonance peaks of nuclear reaction cross-sections fron the ENDF/B-VII.0 data. The black, red, and green lines are the neutron total, capture, and elastic cross-sections, respectively.

IV. CALCULATION, RESULTS, AND DISCUSSION

Calculations were done with a simple analytic calculation model. Consider the geometry shown in Fig. 5,

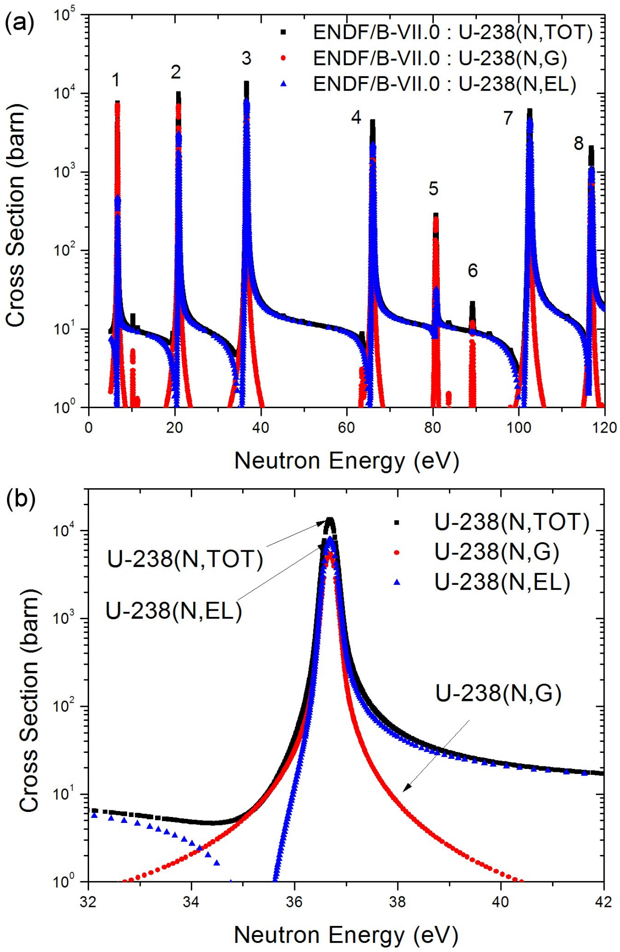

Fig. 4. Resonance peaks of the nuclear reaction for the neutron total, capture, and elastic cross-sections (ENDF/B-VII.) At the neutron energy (a) 6.673 $\sim$ 116.895 eV and (b) 36.68 eV.

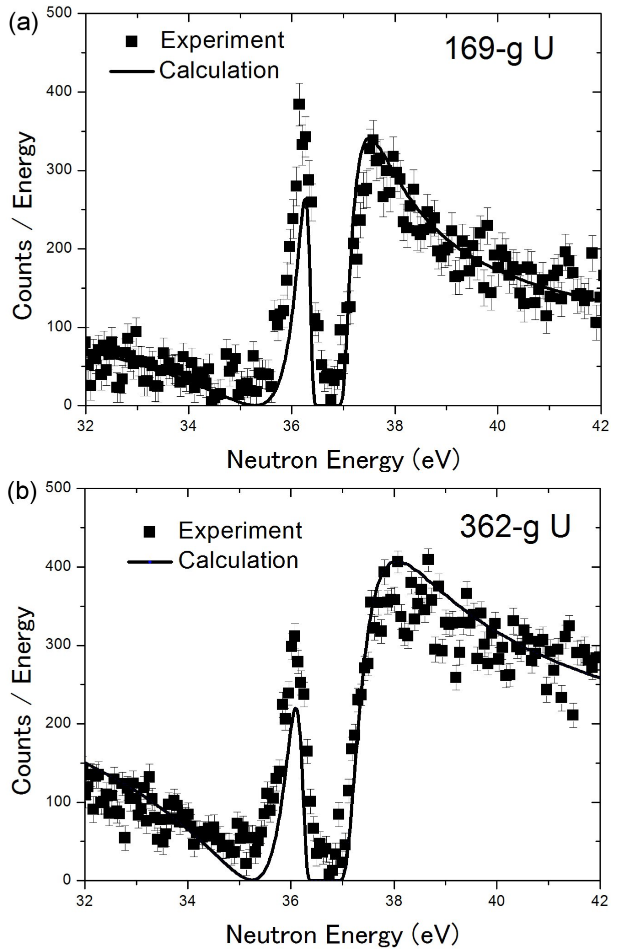

Fig. 6. Experimental and calculated results for neutron scattering from a depleted U sample: (a) 169-g sample and (b) 362-g sample.

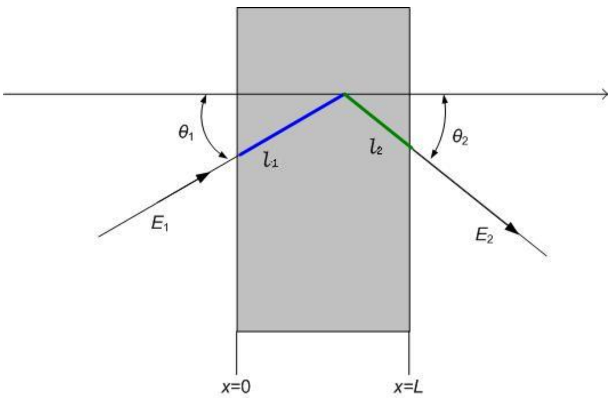

Fig. 5. The Geometry for the neutron scattering calculation.

in which a neutron beam is incident on a slab of thickness L at an angle $\theta 1$ and is scattered towards a neutron detector at angle $\theta 2$. $l1$ and $l2$ are the lengths of the incident and the scattered paths of neutrons in the material, respectively.

The energy relation between the incident neutron energy E_1 and the scattered neutron energy E_2 for a scattering material (atomic mass A) is given by [11]

$$K = \frac{E_1}{E_2} = \frac{(A+1)^2}{A^2 + 2A \cdot J_{cm} + 1} \tag{1}$$

where $J_{cm} = \cos\phi$ the scattering angle ϕ in the center of mass system. The fraction of neutrons of energy E_1 that scatter towards the direction of the detector at angle θ_2 can be calculated by taking into account the attenuation of the neutrons before they reach the collision point, the scattering probability, and the attenuation of the scattered neutrons:

$$dP = \exp[-\Sigma_t(E_1)l_1]\Sigma_s^{Lab}(E_1,\theta)dl_1 \exp[-\Sigma_t(E_2)l_2] \tag{2}$$

where $\Sigma_t(E_1)$ and $\Sigma_t(E_2)$ are the macroscopic total cross sections of incident neutron energy E_1 and scattered neutron energy E_2 , respectively. The macroscopic differential elastic scattering cross section is given by $\Sigma_s^{Lab}(E_1,\theta)$. The scattering cross section is assumed to be isotropic in the center of mass system and can be calculated from the energy-dependent tabulated cross-section by using the $\Sigma_s^{Lab}(E)$ transformation

$$\Sigma_s^{Lab}(E, J_{cm}) = \frac{\Sigma_s^{Lab}(E)}{4\pi} \frac{(A^{-2} + 2A^{-1}J + 1)^{3/2}}{A^{-1}J + 1} \quad (3)$$

The final expression for the scattering probability for a scattering material that contains n atoms is given by

$$P = dE_2 \Sigma_i^n K_i \phi(E_i) \frac{\Sigma_s^{Lab}(E, J_{cm})}{\Sigma_t(E_2) \frac{J_1}{J_2} \Sigma_t(E_i)} \times \left[\exp - \Sigma_t(E_i) \frac{L}{J_2} - \exp - \Sigma_t(E_2) \frac{L}{J_2} \right] \quad (4)$$

where $\phi(E_i)$ is the incident neutron flux, $l_1 = L/J1$ is the and incident neutron path $J_1 = \cos\theta_1$, and $J_2 = \cos\theta_2$.

The measured product of the flux shape and the energy-dependent neutron source was used in calculation. Comparing the measured data and calculations shows discernable differences at the peak, as shown in Fig. 6. The neutron scattering spectrum was calculated by using the energy dependent scattering probability and incident neutron flux of Eq. (4) in the energy range from 32 eV to 42 eV (500 points) with a 0.02-eV bin width.

The calculations were normalized to the experimental data at the peaks near 37.5 eV (169-g sample) and 38.0 eV (362-g sample). The dip in the measured spectrum occurs at the resonance energy and is due to attenuation of the scattered neutrons as they leave the sample and travel towards the detector. These results show that the current calculation underestimates the measured forward scattering intensity. Similar results were obtained for a thicker depleted U sample.

V. CONCLUSIONS

An experimental setup was used to determine the neutron scattering by ^{238}U in the energy range from 5 to 120 eV at a 38.9° forward angle. An accurate calculated neutron scattering spectrum is essential for detailed studies of the resonance peak in the forward scattering.

In the experiment neutron scattering spectrum, the peak of 169-g thin sample was more sharp than the peak of 362-g thick sample. We can expect that the ratio of the peak for the bump of near resonance depend upon sample thickness. Therefore more experimental data of various thickness are needed to get the accurate quantitative ratio of the peak for the bump.

The current calculated neutron scattering spectra are in a good agreement for the peak energy and the shape of bump with experimental spectra. But the calculated intensity of neutron scattering peak does not accurately match the experiment result in the resonance region. Differences in the intensity and the shape around the resonance of the scattered neutron spectrum are evident for forward scattering from thin and thick ^{238}U samples.

Because the total scattering must be preserved in both the calculation and the experiment and because the calculated and experimental forward scatterings were found to be identical, that at other angles is expected to also show differences. Enik *et al.* [6] performed measurements at angles of 25° and 155° for thin and thick ^{238}U samples and reported different shapes for different scattering angles and thicknesses.

Thus, more experiments with different scattering angles and calculation models are needed. Using MCNP with a free gas model and the S(a, b) model [8,9], we can compare the current scattering experiment with more detailed situation. The velocity of the target nucleus is sampled for low-energy (below about 4 eV) neutrons in S(a, b) model.

ACKNOWLEDGMENTS

The authors would like to acknowledge the RPI LINAC operations team, Peter Brand, Mathew Gray, Martin Strock, and Azeddine Kerdoun, for their dedication and help with the setup of the experiment. One of authors (Tae-Ik Ro) is partly supported through the Dong-A University research fund. This research was also supported by the Dong-A University research fund.

REFERENCES

[1] D. K. Olsen, G. de. Saussure, R. B. Perez, E. Z. Silver, F. C. Difilippo, R. W. Ingle and H. Weaver, Nucl. Sci. Eng. **62**, 479 (1977).
[2] T. Miura, M. Baba, M. Ibaraki, T. Win, T. Sanami and Y. Hirasawa, Ann. Nucl. Energy **28**, 937 (2001).
[3] T. Miura, M. Baba, M. Ibaraki, T. Sanami, T. Win, Y. Hirasawa and N. Hirakawa, Ann. Nucl. Energy **27**, 625 (2001).
[4] M. Asghar, C. M. Chaffey and M. C. Moxon, Nucl. Phys. **85**, 305 (1966).
[5] P. Staveloz, F. Poortmans, L. Mewissen and E. Cornelis, Nucl. Sci. Eng. **66**, 349 (1978).
[6] T. L. Enik, L. V. Mitsyna, G. S. Samosvat and V. V. Sinitsa, *ISINN-8 Proceeding* (Dubna, 2000) p. 371.
[7] MCNP, A General Monte Carlo Code for Neutron and Photon Transport, Version 5, LA-UR-05-8617 (2005).
[8] W. Rothenstein and R. Dagan, Annals. Nuclear Energy **25**, 209 (1998).
[9] W. Rothenstein, Annals. Nuclear Energy **31**, 9 (2004).
[10] W. Rothenstein and R. Dagan, Annals. Nuclear Energy, **22**, 723 (1995).
[11] S. E. Liverhant, *Nuclear Reactor Physics* (Wiley, New York, 1960), p. 146